Available online at www.sciencedirect.com
SCIENCE DIRECT
Cement and Concrete Research 36 (2006) 227 – 237
Cement and Concrete Research

A thermodynamic model of dissolution and precipitation of calcium silicate hydrates

Daisuke Sugiyama *, Tomonari Fujita

Nuclear Technology Research Laboratory, Central Research Institute of Electric Power Industry (CRIEPI), 2-11-1, Iwado-kita, Komae-shi, Tokyo 201-8511, Japan

Received 7 September 2005; accepted 12 September 2005

Abstract

A thermodynamic incongruent dissolution/precipitation model of calcium silicate hydrate (C-S-H) is proposed, assuming a binary nonideal solid solution of $Ca(OH)_2$ and SiO_2. Using this model, both dissolution and precipitation of the C-S-H phase, with a continuous change in the Ca/Si ratio of the solid phase, can be predicted. The notable features of the model are its good continuity and simplicity so that calculation can be easily compiled in a calculation code. A series of experiments were carried out. C-S-H precipitates were prepared using two techniques: precipitation by contacting $Ca(OH)_2$ solution with C-S-H gel and hydrolysis in a mixture of Ca and Si solutions. The equilibria in these experiments were predicted well by the proposed model. A calculation using the model also predicted well the dissolution of ordinary Portland cement hydrate with water exchange.

Keywords: Radioactive waste; Calcium silicate hydrate (C-S-H); Dissolution; Precipitation; Thermodynamic model

1. Introduction

Cementitious material, a potential waste packaging and backfilling material for the disposal of radioactive waste, is expected to provide not only a physical barrier to migration but also a chemical containment. In particular, the ability to provide high-pH conditions, which depends on the solubility of the constituent hydrated minerals of cement matrices, is a very important parameter when considering the release of radionuclides from radioactive waste; the solubility is low and the sorption distribution ratio is high for many radioactive species at high pHs.

For the long-term safety assessment of radioactive waste disposal, it is necessary to develop a series of predictive calculation models of the behaviour of the repository system. Several models have been proposed for the incongruent dissolution of calcium silicate hydrate (C-S-H) gel, which is the principal product of hydrated cement phases and mainly determines the pH condition in the near field. Berner [1] described the incongruent solubility behaviour of C-S-H gel by introducing several independent model solids, $Ca(OH)_2$ and CaH_2SiO_4 at a Ca/Si ratio ≥ 1 and CaH_2SiO_4 and SiO_2 at a Ca/Si ratio < 1; solubility products were given as functions of gel composition. Reardon [2] modelled C-S-H gel as xCaO·SiO_2·$x$$H_2O$ and quantified its solubility product as a function of the Ca/Si ratio of the gel. Atkinson et al. [3] described the aqueous solubility of C-S-H gel by assuming that amorphous SiO_2 and $Ca(OH)_2$ can form a solid solution with tobermorite and calculated the equilibrium state of a system by minimising its total free energy. Börjesson et al. [4] modelled C-S-H gel at a Ca/Si ratio ≥ 1 as a nonideal binary solid solution composed of the end members $Ca(OH)_2$ and CaH_2SiO_4 and used a mixing model of the Margules type to account for the nonideality. Rahman et al. [5,6] proposed a model of the dissolution of C-S-H gel by considering a nonideal mixture of binary solid solutions also of the Margules type. Kulik and Kersten [7] described the solubility of Ca and Si in the fully hydrated C-S-H system using two ideal Si-rich C-S-H-(I) and Ca-rich C-S-H-(II) solid solution phases and applying the Gibbs energy minimisation approach, considering the atomistic models of the metastable C-S-H gel structure. Kulik and Kersten suggested that C-S-H gels combine features of both

* Corresponding author. Tel.: +81 3 3480 2111; fax: +81 3 3480 3564.
E-mail address: daisukes@criepi.denken.or.jp (D. Sugiyama).

0008-8846/$ - see front matter © 2005 Elsevier Ltd. All rights reserved.
doi:10.1016/j.cemconres.2005.09.002

sublattice and interstitial mixing of the end members [7]. All models above reproduce the available solubility data for C-S-H gel in water [8–11] reasonably well.

To model cementitious systems, cement materials are sometimes described as assemblages of the constituent minerals: for example, hydrated Portland cement was described as a mixture of portlandite, C-S-H gel, ettringite and some other minerals [1,12]. Then the incongruent dissolution/precipitation of C-S-H gel and the congruent dissolution/precipitation of the constituent hydrated minerals would be discussed and calculated simultaneously. In these cases, therefore, it is appropriate that the reactions are described as simply as possible in the calculation by using a geochemical speciation code to calculate the equilibrium of the complex system as simultaneous equations of the constituent minerals. For the long term in a repository, the high pH is gradually neutralised by interaction with groundwater [13]. To calculate the continuous evolution of the chemistry of cementitious system, it is appropriate that the incongruent dissolution model of C-S-H has continuity over the entire range of Ca/Si ratio in numerical modelling, though some previous models used different sets of model solids at different regions of Ca/Si ratio [1,3,5,6].

In this study, a thermodynamic dissolution and precipitation model of the C-S-H phase is proposed to discuss the aqueous chemistry and the continuous change in the composition of the solid phase of the C-S-H system simultaneously by assuming a simple binary nonideal solid solution of $Ca(OH)_2$ and SiO_2 over the entire range of Ca/Si ratios. Precipitation experiments on C-S-H gel were carried out to discuss the applicability of the proposed model to the safety assessment of radioactive waste disposal. C-S-H precipitates were prepared using two techniques. One was based on hydrolysis in a mixture of Ca and Si solutions and produced homogeneous gels. In the other technique, precipitates were prepared by contacting $Ca(OH)_2$ solution with C-S-H gels having low Ca/Si ratios (0.47, 0.65 and 0.9). The dissolution of ordinary Portland cement (OPC) hydrate was also discussed in the context of the proposed model.

2. Modelling

2.1. Description of C-S-H phase

C-S-H gel is the principal product of hydrated cement phases. It has a variable composition and a wide range of Ca/Si ratios, and dissolves incongruently. Although C-S-H gel is not fully understood structurally, it has been shown that it has a nanostructure and demonstrates a structural similarity to tobermorite [14], which is a $CaO–SiO_2–H_2O$ mineral. Tobermorite has a layer structure in which each layer consists of a central part of empirical formula CaO_2; all the oxygen atoms of the Ca–O layer are shared with Si–O chains and additional Ca^{2+} and OH^- ions are suggested to be present in the interlayer region of the structure [14]. C-S-H gel can be fundamentally described as a structure that consists of Si–O (SiO_4 tetrahedra) chains and interlayer Ca–O (Ca^{2+} and OH^-). In reality, C-S-H gels have a highly disordered structure. It is, therefore, possible to describe the activities of $Ca(OH)_2$ and SiO_2 in C-S-H gel separately and represent the chemistry of C-S-H by a simple system of the model solids, $Ca(OH)_2$ and SiO_2.

In this study, C-S-H gel is modelled as a simple binary nonideal solid solution of $Ca(OH)_2$ and SiO_2 at all Ca/Si ratios of the solid C-S-H phase based on the discussion above, to discuss the aqueous chemistry and change in the composition of the solid phase of the C-S-H system simultaneously. This model can be easily employed in thermodynamic geochemical calculations because of its continuity and simplicity. And the good continuity enables to compile the iterative numerical calculations of incongruent dissolution/precipitation (as discussed in Section 4).

2.2. Thermodynamic modelling

The thermodynamic modelling of the incongruent dissolution/precipitation of C-S-H gel is based on the mixing model proposed by Guggenheim [15]. The model would describe C-S-H gel as a binary nonideal solid solution. Excess free energy can be expressed by a power series of the mole fractions of the end members. In the present model, the expression becomes

$$G_{\text{excess}} = X_1X_2[A_0 + A_1(X_1 - X_2) + A_2(X_1 - X_2)^2 + A_3(X_1 - X_2)^3 + \cdots], \quad (1)$$

where

X_i is the mole fraction of the end member i;
A_j is a parameter that is not dependent on composition but varies with temperature and pressure.

If the series is terminated after three terms, the change in Gibbs free energy in the formation of the solid solution is represented as

$$\Delta_f G^0_{SS} = X_1\Delta_f G^0_1 + X_2\Delta_f G^0_2 + RT(X_1 \ln X_1 + X_2 \ln X_2) + X_1X_2[A_0 + A_1(X_1 - X_2) + A_2(X_1 - X_2)^2]. \quad (2)$$

$\Delta_f G^0$ is also given by

$$\Delta_f G^0 = -RT\ln K. \quad (3)$$

By substituting Eq. (3) into Eq. (2), log K for each end member can be written as a function of the mole fraction of the end member, as follows:

For end member 1,

$$\log K_{SS-1} = X_1 \log K_{10} - X_1 \log X_1 + X_1X_2\left[A'_{10} + A'_{11}(X_1 - X_2) + A'_{12}(X_1 - X_2)^2\right]. \quad (4)$$

For end member 2,

$$\log K_{SS-2} = X_2 \log K_{20} - X_2 \log X_2 + X_1X_2\left[A'_{20} + A'_{21}(X_2 - X_1) + A'_{22}(X_2 - X_1)^2\right]. \quad (5)$$

where K_{i0} is the solubility product of pure end member i, and $A'_{ij} = -\frac{A_{ij}}{2.303RT}$.

By a conditional constant approach [16], the solubility product of each end member can be described as

$$K_{SS-i} = X_i f_i K_{i0}, \tag{6}$$

where f_i is the activity coefficient of end member i in the solid solution.

Then,

$$\log K_{SS-i} = \log(X_i K_{i0}) + \log f_i. \tag{7}$$

By comparing Eq. (7) with Eqs. (4) and (5), $\log f_i$ can be written as follows:

For end member 1,

$$\log f_1 = (X_1 - 1)\log K_{10} - (X_1 + 1)\log X_1 + X_1 X_2\left[A'_{10} + A'_{11}(X_1 - X_2) + A'_{12}(X_1 - X_2)^2\right]. \tag{8}$$

For end member 2,

$$\log f_2 = (X_2 - 1)\log K_{20} - (X_2 + 1)\log X_2 + X_1 X_2\left[A'_{20} + A'_{21}(X_2 - X_1) + A'_{22}(X_2 - X_1)^2\right]. \tag{9}$$

In the present model, end members 1 and 2 are SiO_2 and $Ca(OH)_2$, respectively. Thus, X_1 and X_2 are

$$X_1 = \frac{1}{1 + (\mathrm{Ca/Si})} \tag{10}$$

$$X_2 = \frac{(\mathrm{Ca/Si})}{1 + (\mathrm{Ca/Si})}. \tag{11}$$

Substituting Eqs. (10) and (11) into Eqs. (8) and (9), respectively, gives the following:

For end member 1 (SiO_2, denoted by subscript s),

$$\log f_s = -\frac{(\mathrm{Ca/Si})}{1 + (\mathrm{Ca/Si})}\log K_{s0} - \frac{2 + (\mathrm{Ca/Si})}{1 + (\mathrm{Ca/Si})}\log\frac{1}{1 + (\mathrm{Ca/Si})} + \frac{(\mathrm{Ca/Si})}{\{1 + (\mathrm{Ca/Si})\}^2}\cdot\left[A'_{s0} + A'_{s1}\left\{\frac{1 - (\mathrm{Ca/Si})}{1 + (\mathrm{Ca/Si})}\right\} + A'_{s2}\left\{\frac{1 - (\mathrm{Ca/Si})}{1 + (\mathrm{Ca/Si})}\right\}^2\right]. \tag{12}$$

For end member 2 ($Ca(OH)_2$, denoted by subscript c),

$$\log f_c = -\frac{1}{1 + (\mathrm{Ca/Si})}\log K_{c0} - \frac{1 + 2(\mathrm{Ca/Si})}{1 + (\mathrm{Ca/Si})}\log\frac{(\mathrm{Ca/Si})}{1 + (\mathrm{Ca/Si})} + \frac{(\mathrm{Ca/Si})}{\{1 + (\mathrm{Ca/Si})\}^2}\cdot\left[A'_{c0} + A'_{c1}\left\{\frac{(\mathrm{Ca/Si}) - 1}{1 + (\mathrm{Ca/Si})}\right\} + A'_{c2}\left\{\frac{(\mathrm{Ca/Si}) - 1}{1 + (\mathrm{Ca/Si})}\right\}^2\right]. \tag{13}$$

If f_s and f_c are given, the solubility products of the end members can be calculated using Eq. (6).

2.3. Determination of empirical parameters

The saturation index of end member i that describes the saturation state is calculated using

$$\mathrm{SI}_i = \log\frac{\mathrm{IAP}_i}{K_{i0}}, \tag{14}$$

where IAP_i is the ion activity product of end member i.

If the solid solution is in equilibrium with an aqueous phase, the activity of end member i in the solid solution can be expressed as [4]

$$a_i^{\text{solid solution}} = \frac{\mathrm{IAP}_i}{K_{i0}}. \tag{15}$$

Eqs. (14) and (15) yield

$$a_i^{\text{solid solution}} = 10^{\mathrm{SI}_i}. \tag{16}$$

The activity is also described as

$$a_i^{\text{solid solution}} = f_i X_i. \tag{17}$$

The saturation index of each end member at various Ca/Si ratios at 25 °C was calculated using the available

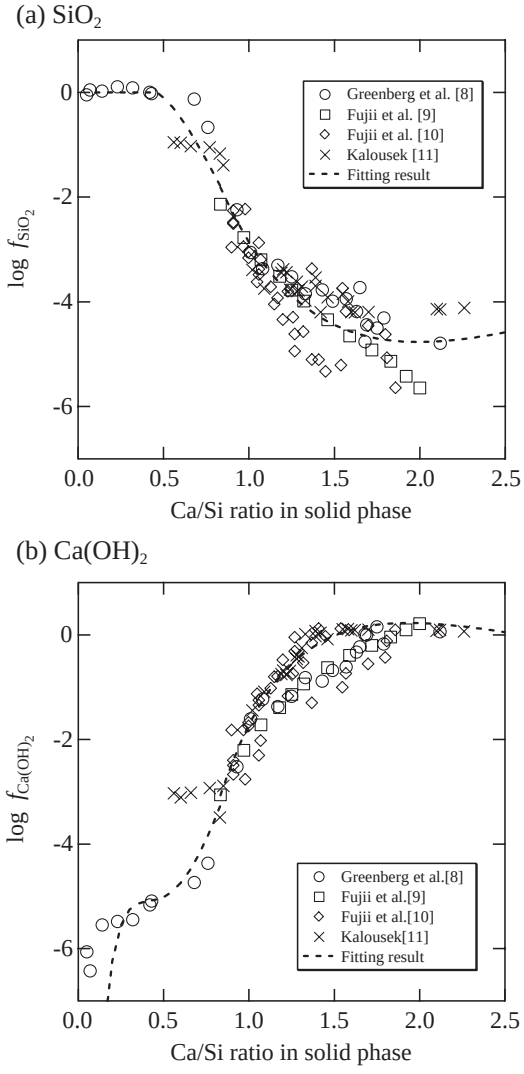

Fig. 1. Activity coefficient of end member as a function of Ca/Si ratio: (a) SiO_2 and (b) $Ca(OH)_2$.

Table 1
Fitted values of empirical parameters at 25 °C

End member	SiO_2			$Ca(OH)_2$		
A_{ij}	A'_{s0}	A'_{s1}	A'_{s2}	A'_{c0}	A'_{c1}	A_{c2}
$Ca/Si \leq 0.833$	−18.623	57.754	−58.241	37.019	36.724	164.17
$Ca/Si > 0.833$	−18.656	49.712	25.033	36.937	7.8302	−50.792

solubility data for C-S-H gel [8–11] with the geochemical code HARPHRQ [17]. The thermodynamic database HATCHES [18] Ver. NEA14 was used in the calculations. The Davies equation was used for ionic strength correction to calculate the saturation index. The SI_i values obtained were then converted to activities using Eq. (16) and the activity coefficients (f_i) were calculated; $\log f_i$ as a function of the Ca/Si ratio of the C-S-H gel solid phase is shown in Fig. 1.

As mentioned above, C-S-H gel has a structural similarity to tobermorite and some previous models were based on the assumption that an intermediate compound having a composition close to that of tobermorite (Ca/Si ratio = 0.833) is the end member of the C-S-H solid solution [3,9]. In the present model, therefore, the fitting calculation for $\log f_i$ of the end members SiO_2 and $Ca(OH)_2$ was carried out at a Ca/Si ratio > 0.833 and a Ca/Si ratio ≤ 0.833 by the least-squares method. The fitted empirical parameters are shown in Table 1 and the fitted curves are shown in Fig. 1. There is good continuity in the fitted curves over the entire range of Ca/Si ratio.

$\log f_s$ increases as Ca/Si ratio decreases and $\log f_s = 0$ at a Ca/Si ratio = 0.461. At very low Ca/Si ratios, the composition of C-S-H is close to that of amorphous SiO_2 [1,14]. Thus, at a Ca/Si ratio ≤ 0.461, the end member SiO_2 is assumed to be an ideal end member in the solid solution and $\log f_s = 0$. Faucon et al. [19] suggested that the layer in the tobermorite-type structure containing calcium atoms is progressively occupied by additional calcium atoms as the Ca/Si ratio exceeds 0.66. This might account for the pronounced change in the slope of f_s at a Ca/Si ratio around 0.461 as shown in Fig. 1(a).

It is found that $\log K_c$ for the dissolution of the end member $Ca(OH)_2$ increases as Ca/Si ratio increases and is the same as that for pure $Ca(OH)_2$ at a Ca/Si ratio = 1.755. From the available solubility data [8–11], the calcium concentration in the C-S-H equilibrated solution was approximately 2×10^{-2} mol dm^{-3} at a Ca/Si ratio > 1.8, which is very close to the solubility limit of pure $Ca(OH)_2$. This suggests that pure

Table 2
Conditional solubility constants of model solids as functions of Ca/Si ratio at 25 °C

Ca/Si ratio	Conditional $\log K_i$
$0 < Ca/Si \leq 0.461$	$\log K_s = \log\left[K_{s0}\cdot\left\{\frac{1}{(Ca/Si)+1}\right\}\right]$
	$\log K_c = \frac{(Ca/Si)}{1+(Ca/Si)}\cdot\log K_{c0} - \frac{(Ca/Si)}{1+(Ca/Si)}\cdot\log\left(\frac{(Ca/Si)}{1+(Ca/Si)}\right) + \left[\frac{(Ca/Si)}{\{1+(Ca/Si)\}^2}\right]\cdot\left[37.019 + 36.724\cdot\left\{\frac{(Ca/Si)-1}{1+(Ca/Si)}\right\} + 164.17\cdot\left\{\frac{(Ca/Si)-1}{1+(Ca/Si)}\right\}^2\right]$
$0.461 < Ca/Si \leq 0.833$	$\log K_s = \frac{1}{1+(Ca/Si)}\cdot\log K_{s0} - \frac{1}{1+(Ca/Si)}\cdot\log\left(\frac{1}{1+(Ca/Si)}\right) + \left[\frac{(Ca/Si)}{\{1+(Ca/Si)\}^2}\right]\cdot\left[-18.623 + 57.754\cdot\left\{\frac{1-(Ca/Si)}{1+(Ca/Si)}\right\} - 58.241\cdot\left\{\frac{1-(Ca/Si)}{1+(Ca/Si)}\right\}^2\right]$
	$\log K_c = \frac{(Ca/Si)}{1+(Ca/Si)}\cdot\log K_{c0} - \frac{(Ca/Si)}{1+(Ca/Si)}\cdot\log\left(\frac{(Ca/Si)}{1+(Ca/Si)}\right) + \left[\frac{(Ca/Si)}{\{1+(Ca/Si)\}^2}\right]\cdot\left[37.019 + 36.724\cdot\left\{\frac{(Ca/Si)-1}{1+(Ca/Si)}\right\} + 164.17\cdot\left\{\frac{(Ca/Si)-1}{1+(Ca/Si)}\right\}^2\right]$
$0.833 < Ca/Si < 1.755$	$\log K_s = \frac{1}{1+(Ca/Si)}\cdot\log K_{s0} - \frac{1}{1+(Ca/Si)}\cdot\log\left(\frac{1}{1+(Ca/Si)}\right) + \left[\frac{(Ca/Si)}{\{1+(Ca/Si)\}^2}\right]\cdot\left[-18.656 + 49.712\cdot\left\{\frac{1-(Ca/Si)}{1+(Ca/Si)}\right\} + 25.033\cdot\left\{\frac{1-(Ca/Si)}{1+(Ca/Si)}\right\}^2\right]$
	$\log K_c = \frac{(Ca/Si)}{1+(Ca/Si)}\cdot\log K_{c0} - \frac{(Ca/Si)}{1+(Ca/Si)}\cdot\log\left(\frac{(Ca/Si)}{1+(Ca/Si)}\right) + \left[\frac{(Ca/Si)}{\{1+(Ca/Si)\}^2}\right]\cdot\left[36.937 + 7.8302\cdot\left\{\frac{(Ca/Si)-1}{1+(Ca/Si)}\right\} - 50.792\cdot\left\{\frac{(Ca/Si)-1}{1+(Ca/Si)}\right\}^2\right]$
$1.755 \leq Ca/Si$	$\log K_s = -7.853$ $\log K_c = 22.81$ (= $\log K_{c0}$)

HATCHES Ver. NEA14 [18]

$SiO_2 : SiO_2 + 2H_2O = H_4SiO_4 \quad \log K_{s0} = -2.710$

$Ca(OH)_2 : Ca(OH)_2 + 2H^+ = Ca^{2+} + 2H_2O \quad \log K_{c0} = 22.81.$

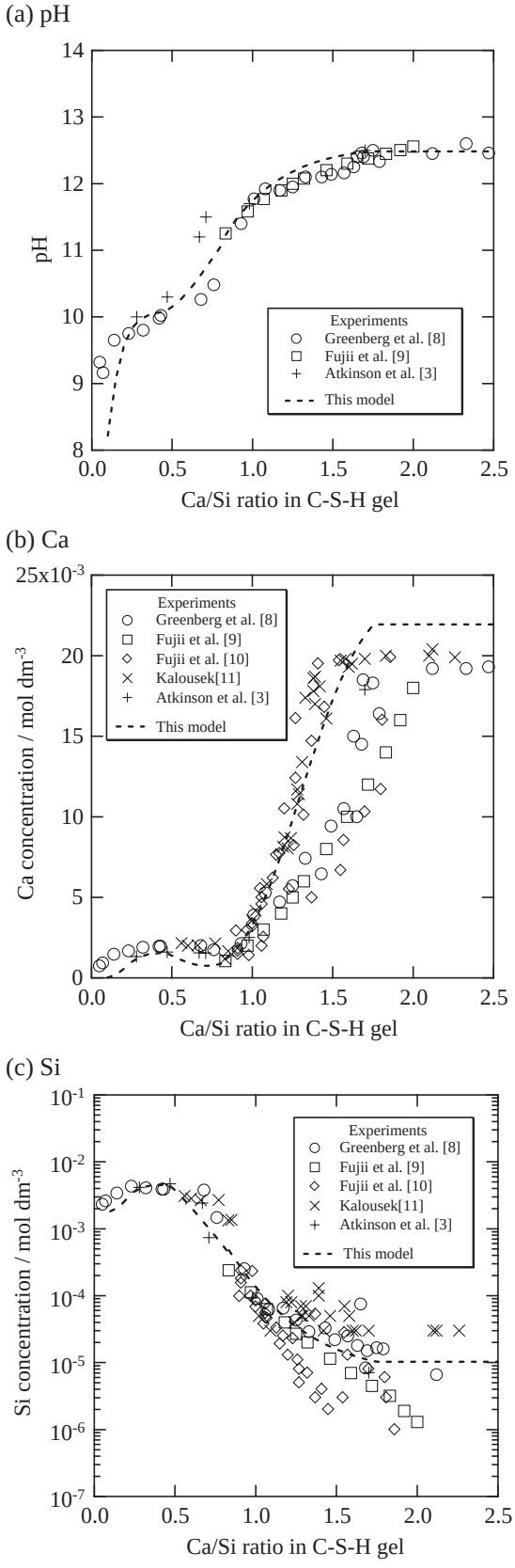

Fig. 2. Measured and predicted compositions of liquid phase in equilibrium with C-S-H gel as functions of Ca/Si ratio in solid phase: (a) pH, (b) Ca concentration and (c) Si concentration.

$Ca(OH)_2$ separates and coexists with C-S-H gel. Therefore, the log K for each end member is fixed at log $K_c = 22.81$ (the same as that for pure $Ca(OH)_2$ in the HATCHES database) and log $K_s = -7.853$ (this value is calculated at a Ca/Si ratio = 1.755) at a Ca/Si ratio $\geq$ 1.755.

The calculated log K values for the end members are summarised in Table 2. In the present model, it is assumed that C-S-H is a nonideal binary solid solution of $Ca(OH)_2$ and SiO_2 at $0 < Ca/Si < 1.755$ (at a Ca/Si ratio ≤ 0.461, the end member SiO_2 is an ideal end member) and $Ca(OH)_2$ is separated and coexists with the C-S-H gel (Ca/Si = 1.755) at Ca/Si $\geq$ 1.755. It should be noted that the equations in Table 2 are valid only in conjunction with the thermodynamic database used for fitting. If another or modified thermodynamic data were employed, log K as a function of Ca/Si ratio should be recalculated using the same procedure described above.

Solubility calculation for C-S-H was carried out using the conditional solubility constants shown in Table 2 and the result is shown in Fig. 2. This model predicts well the literature data.

3. Experimental

3.1. Precipitation of C-S-H

We observed and analysed the precipitation of C-S-H using two procedures: (a) calcium was precipitated by contacting $Ca(OH)_2$ solution with low Ca/Si solid C-S-H and the change in the composition of the solid was measured (precipitation method) and (b) C-S-H gel was prepared in a mixture of Ca and Si solutions based on hydrolysis (coprecipitation method). These experiments are designed to discuss the applicability of the proposed model to the evolution of the composition (Ca/Si ratio) and precipitation of C-S-H.

3.1.1. Precipitation method

The experimental methodology is shown in the flowsheet of Fig. 3(a). C-S-H solids with low Ca/Si ratios (0.47, 0.65 and 0.9) were prepared by mixing an appropriate amount of CaO with amorphous silica in distilled water and aging the mixture for more than 7 days. The hydrated samples were dried at room temperature in a vacuum desiccator above silica gel, then crushed and passed through a 250 μm sieve. Ca solution was prepared by equilibrating $Ca(OH)_2$ solid with distilled water for more than 3 days and filtering the mixture through a 0.45 μm membrane filter. The measured Ca concentration in the filtrate was 1.6×10^{-2} mol dm^{-3}. Then the previously prepared C-S-H gels were contacted with the Ca solution at a liquid : solid ratio of 100 : 1 in an Ar-filled ($O_2 < 2$ ppm) glovebox. The supernatants and precipitates were analysed after various time intervals up to 61 days when the experiments appeared to have reached a steady state with a constant pH. Ca and Si concentrations in the solution were measured after filtration through a 0.45 μm filter by atomic adsorption and ICP-AES, respectively. The precipitates were dried and analysed by X-ray diffraction (XRD) and differential thermal analysis (DTA) and no phases other than C-S-H gel were identified in the precipitates.

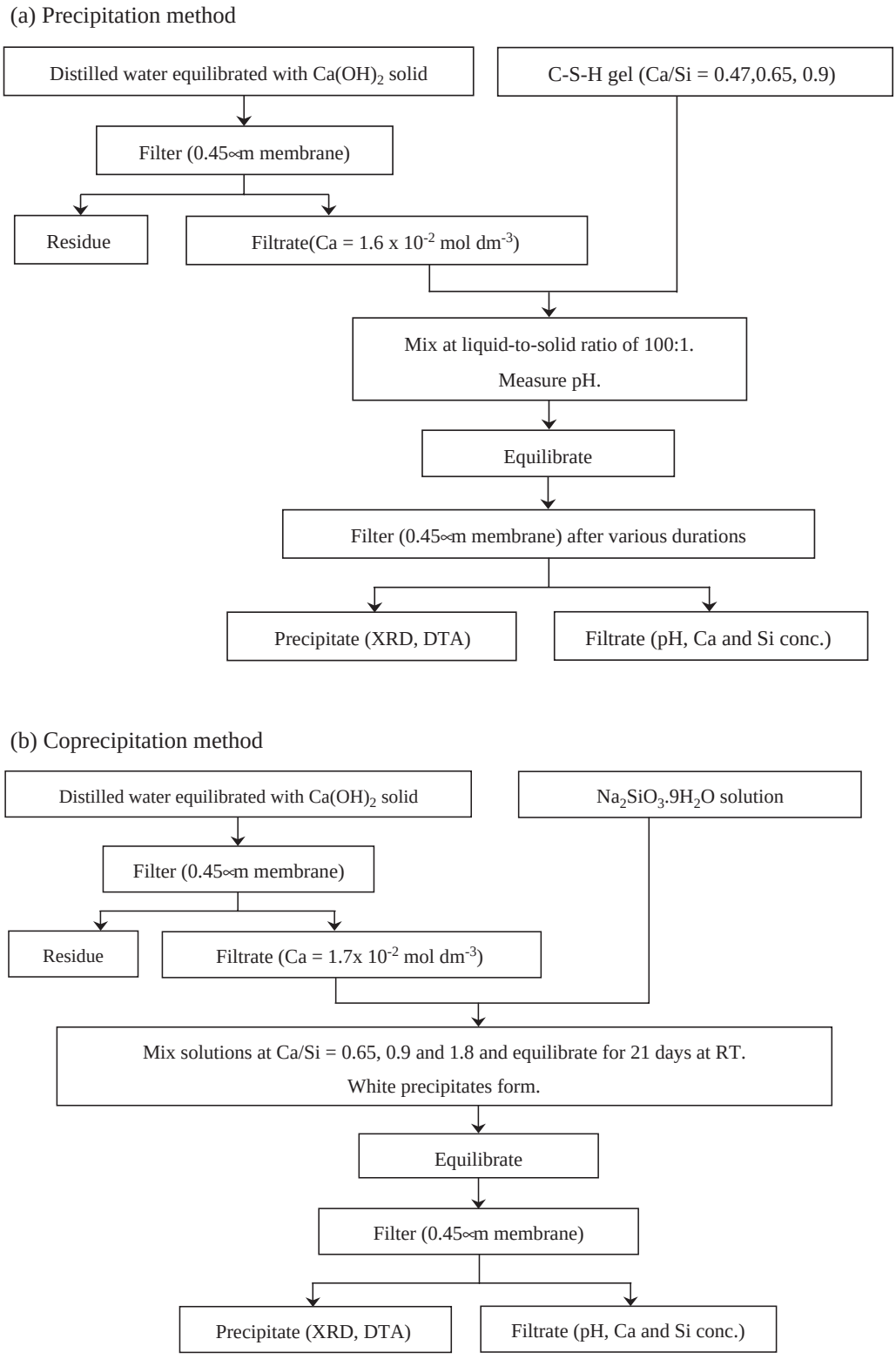

Fig. 3. Experimental methodology.

The results of the analysis of the liquid phase by the precipitation method are shown in Fig. 4(a)–(c). It was observed that Ca concentration decreased from 1.6×10^{-2} to 7×10^{-3} mol dm^{-3} for C-S-H 0.9 (initial Ca/Si=0.9), and decreased to 1×10^{-3} mol dm^{-3} for C-S-H 0.47 and 0.65 (initial Ca/Si=0.47 and 0.65). These suggest that some Ca precipitated from the solution phase and the precipitated Ca was incorporated into the C-S-H structure and Ca/Si ratio has evolved. The Ca/Si ratio of each equilibrated C-S-H solid calculated by considering material balance was higher than that of each initial C-S-H sample (0.47 increased to 0.62, 0.65 increased to 0.82 and 0.9 increased to 1.0) as shown in Fig. 4(a)–(c). These reactions may

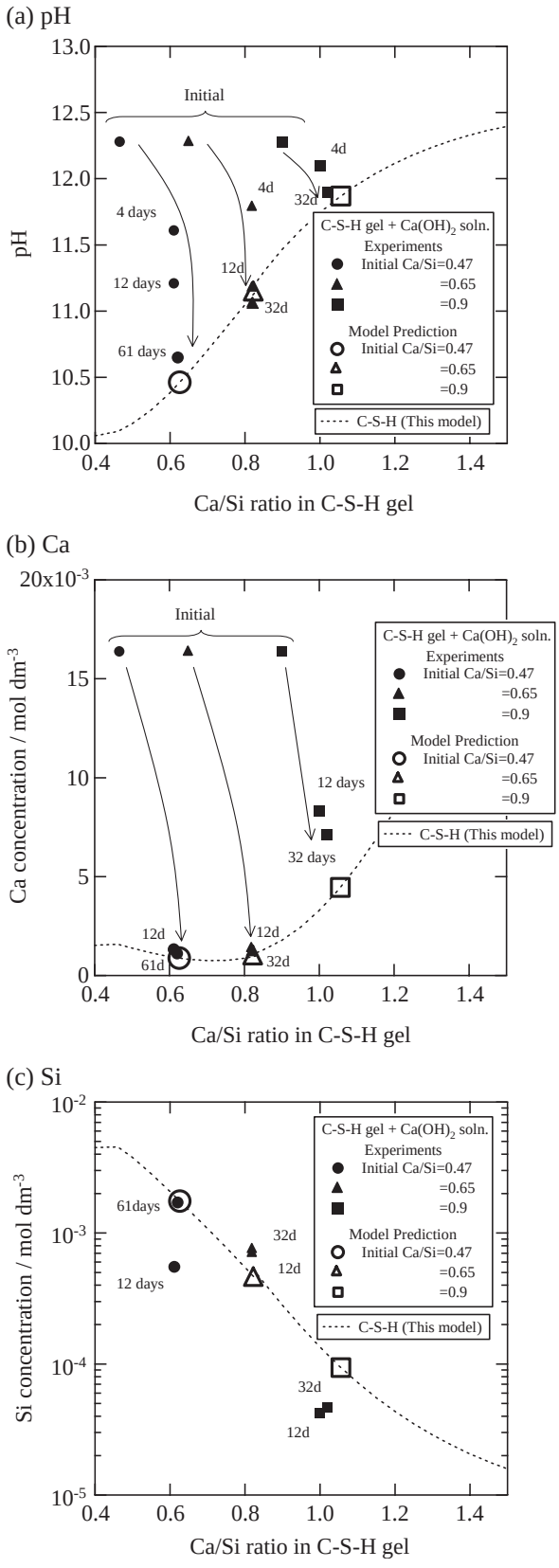

Fig. 4. Measured and predicted compositions of equilibrated liquid phase in C-S-H precipitation experiments (C-S-H+$Ca(OH)_2$ solution): (a) pH, (b) Ca concentration and (c) Si concentration.

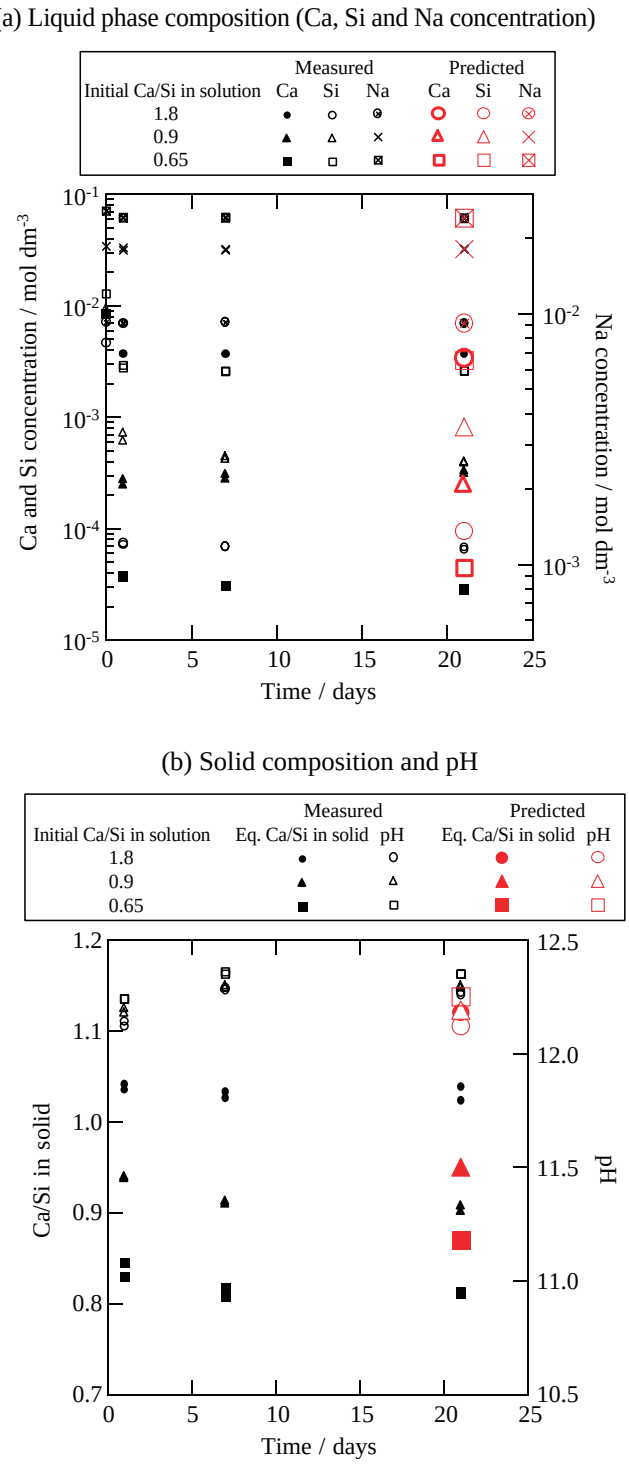

Fig. 5. Liquid and solid phase compositional variations with time in C-S-H coprecipitation experiments.

have proceeded with the dissolution of some Si of C-S-H and reprecipitation of C-S-H. Fig. 4(c) shows that more Si must dissolve for C-S-H with a lower Ca/Si ratio, therefore longer times are needed to reach equilibrium for C-S-H with a lower Ca/Si ratio. It is also noted that precipitated Ca diffuses into the C-S-H solid and that diffusion may be the rate-determining step in reaching a steady state.

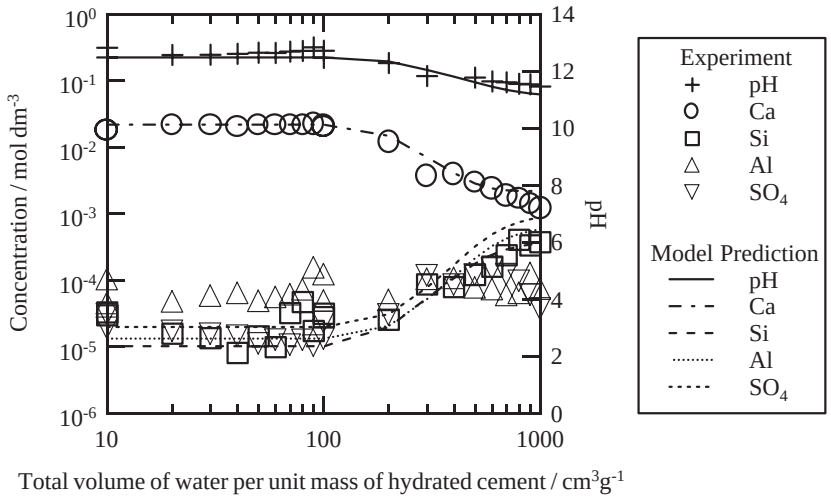

Fig. 6. Measured and predicted composition of the liquid phase in the OPC hydrate dissolution experiment.

3.1.2. Coprecipitation method

The experimental methodology is shown in the flowsheet of Fig. 3(b). Ca solution for the coprecipitation method was prepared by equilibrating $Ca(OH)_2$ powder with distilled water in an Ar-filled glovebox and filtering the mixture through a 0.45 μm filter. The measured Ca concentration in the filtrate was 1.7×10^{-2} mol dm^{-3}. The prepared Ca solution was mixed with $Na_2SiO_3{\cdot}9H_2O$ solution with Ca/Si ratios of 1.8, 0.9 and 0.65. White precipitates formed immediately during mixing of the solutions and persisted in the same solution aged up to 21 days at room temperature. The supernatants and precipitates were analysed in the same manner as that in the precipitation method. No phases other than C-S-H gel were identified in the precipitates by XRD and DTA. These experiments were carried out in duplicate.

The results of the analysis of the liquid phase in the coprecipitation method are shown in Fig. 5. All experiments reached equilibrium after 21 days. It should be noted that pH, and Ca and Si concentrations were different from those for the solubility of C-S-H with the same Ca/Si ratio in pure water. The coexisting Na concentrations (shown in Fig. 5) buffered the pH around 12.3 and restricted Ca solubility. The results suggest the common ion effect and are comparable with those measured by Macphee et al. [20] in higher concentrations (0.25~0.8 M) of NaOH solution at lower L/S ratios; Ca concentration in solution decreased and Si concentration increased, as Na concentration increased.

3.2. Dissolution of OPC hydrate

A hydrated OPC solid sample was prepared at a high water–cement ratio of 0.45, aged for 28 days, crushed and passed through a 250 μm sieve. The powdered OPC hydrate was contacted with distilled water at liquid : solid ratios of 10 : 1 and 100 : 1. It is noted that hydration should have continued during the dissolution experiments since a small amount of unhydrated

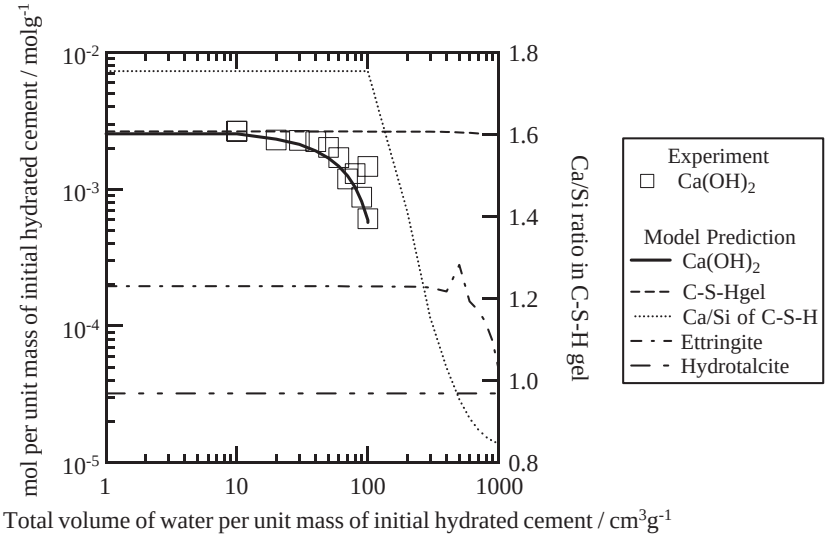

Fig. 7. Measured and predicted mineral composition in the solid phase in the OPC hydrate dissolution experiment.

Table 3
Oxide composition of OPC

[wt.%]							
SiO_2	Al_2O_3	Fe_2O_3	CaO	MgO	SO_3	Na_2O	K_2O
21	5	3	65	1	2	0.3	0.3

phases was observed in the initial powdered OPC hydrate by XRD. The influence of unhydrated phases should have been minimised in the dissolution equilibration period because the powdered OPC sample (<250 μm) was analysed again by XRD after the contact with water for 20 days and was almost hydrated. After 20 days of equilibration, the liquid and solid phases were separated by centrifugation and filtration through a 0.45 μm filter. The supernatants and precipitates were analysed as described above. Then the precipitates were recontacted with fresh distilled water at liquid : solid ratios of 10 : 1 and 100 : 1. This procedure was repeated ten times. The experiment was carried out in duplicate. The results of the analysis of the liquid phase are shown in Fig. 6. The measured amount of $Ca(OH)_2$ in the solid phase by DTA is shown in Fig. 7. In these figures, averaged values are given to avoid congestion. It is noted that the agreement between the duplicate measurements at each point was very good.

At an accumulated liquid : solid (L/S) ratio ≤ 200, pH and Ca concentration were very close to the solubility of $Ca(OH)_2$, showing that $Ca(OH)_2$ dominated the equilibrium between OPC hydrate and water. As the L/S ratio became larger than 200, pH and Ca concentration decreased and Si concentration increased. At $L/S > 200$, $Ca(OH)_2$ was not observed in the solid phase. These suggest that $Ca(OH)_2$ in the OPC hydrate dissolved at $L/S > 200$ and the Ca/Si ratio of C-S-H decreased due to the incongruent dissolution of C-S-H.

4. Applicability of model

The equilibria in the series of experiments described in Section 3 are calculated using the proposed model and the modelling results are compared with the experimental data. It should be noted that we discuss the applicability of the proposed C-S-H dissolution/precipitation model to the safety assessment of radioactive waste in this paper. The details of the other reactions, e.g., sorption of Na onto C-S-H, are not included in the present calculations.

4.1. C-S-H precipitation

For the precipitation method, the initial C-S-H with the specified quantity and Ca/Si ratio and the $Ca(OH)_2$ solution used in the experiments were considered in the modelling calculations. In the first step of the calculation, the quantities of dissolved/precipitated end member solids were calculated for use in the second (next) step. The conditional solubility constants of the end members were recalculated using the equations given in Table 2. This series of calculation steps was repeated until stable solid and liquid phase quantities and compositions were obtained, that is, the system reached equilibrium. It should be noted that good continuity and simplicity over the entire range of Ca/Si ratio of the proposed model enable the iterative calculations in numerical modelling for equilibrium of the C-S-H precipitation experiments.

The modelling results for the precipitation experiments are shown in Fig. 4(a)–(c). The calculations using the proposed model predicted the experiments reasonably well, considering the uncertainty of the solubility data.

In the coprecipitation experiments, there was no solid in the initial solutions. In the modelling calculation using the proposed model, however, some arbitrary input of the initial quantity and composition (Ca/Si ratio) of the solid phase should have been given to initiate the equilibrium calculation. Therefore, in the first step of the calculation, it was assumed that an appropriate amount of C-S-H with a Ca/Si ratio = 1.0 precipitated in the liquid phase during the mixing of the initial solutions. The quantities of dissolved/precipitated end members were estimated and the iterative thermodynamic calculations for equilibrium were carried out by a procedure similar to that used in the precipitation method. The Ca/Si ratio of 1.0 was given for the assumed initial composition of the precipitation since the measured equilibrated Ca/Si ratios of the C-S-H solids were around 1.0 as shown in Fig. 5(b). It should be noted that the assumed composition of the initial precipitation does not affect the calculation results and the routine of iterative calculations gives an equilibration of the system. The measured concentration of Na as an aqueous species was added in the input of the calculation to consider the common ion effect referred to earlier, though sorption of Na onto C-S-H gel was not modelled in the calculation.

The modelling results for the coprecipitation experiments are shown in Fig. 5. The aqueous compositions were well predicted by considering the common ion effect of Na, although the calculated Ca/Si ratios of the solid phase were slightly higher than the measured values.

From the above discussion, we can conclude that the proposed model reasonably well predicts the change of composition of C-S-H that was observed quantitatively in the precipitation experiments. The model has a good continuity and simplicity, which enables the dissolution/precipitation in the C-S-H system to be estimated by iterative calculations.

4.2. Dissolution of OPC hydrate

The mineral composition of the OPC hydrate was derived by an approach based on that described by Glasser et al. [21]

Table 4
Calculated mineral composition in OPC hydrate

[mol kg^{-1}]			
Hydrotalcite	Ettringite	C-S-H gel ($1.755CaO{\cdot}SiO_2{\cdot}1.755H_2O$[a])	$Ca(OH)_2$
0.031	0.20	2.6	2.8

[a] The formula of C-S-H is given by the model proposed in this study.

Table 5
Thermodynamic data for dissolution of ettringite and hydrotalcite given in HATCHES NEA14 [18]

Mineral	Reaction	log K_{sp} (I=0)
Ettringite	$Ca_6Al_2(SO_4)_3(OH)_{12}\cdot 26H_2O = 6Ca^{2+} + 2Al^{3+} + 3SO_4^{2-} - 12H^+ + 38H_2O$	57.00
Hydrotalcite	$Mg_4Al_2O_{17}H_{20} + 14H^+ = 4Mg^{2+} + 2Al^{3+} + 17H_2O$	75.34

with some modifications. The chemical composition of OPC used in this study is shown in Table 3.

Step 1. All the MgO was assumed to be incorporated into hydrotalcite. The inventory of Al_2O_3 was adjusted accordingly.
Step 2. SiO_2 was assumed to be taken up by C-S-H phase with Ca/Si=1.755. C-S-H was described by the model proposed in this study.
Step 3. The amount of $Ca(OH)_2$ was estimated by the DTA analysis of the OPC hydrate sample used in the OPC dissolution experiment in this study.
Step 4. The remaining CaO was assumed to be taken up by ettringite, which was observed by XRD. All the remaining Al_2O_3 was assumed to be amorphous alumina gel or taken up by some phases (e.g., C-A-S-H gel), though excess Al is not included in the following modelling calculations.

The mineral composition of the OPC hydrate calculated by the method above is shown in Table 4. Simultaneous equations, including the reactions of C-S-H described using the present model, ettringite and hydrotalcite, were solved by a geochemical calculation code. The dissolution of ettringite and that of hydrotalcite were assumed to be congruent. The thermodynamic data for these minerals given in HATCHES NEA14, shown in Table 5, were used and included in a single input together with C-S-H in the calculation and the simultaneous equations were solved. In the calculation, the quantities of dissolved/precipitated C-S-H end member solids, ettringite and hydrotalcite were calculated so that the quantities and compositions of solid and liquid phases that would be used in the next step could be estimated. The conditional solubility constants of the end members of C-S-H were recalculated using the equations given in Table 2. The series of calculation steps was repeated until the system (solid and liquid phases) reached equilibrium. It should be noted that the sorption of Al and SO_4 onto C-S-H and precipitation of any other solids are not included in the calculations. Rahman et al. [22] studied the dissolution phenomena of C-S-H and ettringite and suggested the substitutions of $Al(OH)_4^-$ and SO_4^{2-} with Si tetrahedra in the structure of C-S-H, but the interaction mechanism between C-S-H and ettringite has not yet quantitatively studied.

The calculation results for the dissolution experiments on the OPC hydrate are shown in Figs. 6 and 7. The modelling calculation predicted well the experimental results for pH, and Ca and Si concentrations in solution and $Ca(OH)_2$ concentration in the solid phase. The level of agreement between the modelling calculation and the measured values of Al and SO_4 concentrations is reasonably good. We can conclude that the proposed model describes well the equilibrium of the OPC hydrate with water within Ca/Si ratios at which the C-S-H phase dominates the dissolution of the OPC hydrate.

5. Conclusions

A thermodynamic incongruent dissolution/precipitation model of C-S-H gel is proposed, assuming a binary nonideal solid solution of $Ca(OH)_2$ and SiO_2.

A series of dissolution experiments were carried out to discuss the applicability of the model to the safety assessment of radioactive waste disposal. C-S-H precipitates were prepared by hydrolysis in a mixture of Ca and Si solutions to produce homogeneous gels and by precipitation of Ca onto the C-S-H solid contacting with $Ca(OH)_2$ solution. Leaching experiment of OPC hydrate with water exchanges was also carried out.

The proposed model predicts well the equilibria of the precipitation/dissolution in the experiments. The prediction is accomplished by a series of calculations in which the quantities of the dissolved/precipitated end members and mineral are calculated stepwisely so that the quantities and compositions of the solid and liquid phases and the conditional solubility constants used in the next step can be estimated. Because of the continuity and simplicity of the model, the calculation can be compiled in a computer thermodynamic calculation code. Therefore, this model is appropriate for the safety assessment calculations on cementitious repository system.

References

[1] U.R. Berner, Waste Manage. 12 (1992) 201.
[2] E.J. Reardon, Waste Manage. 12 (1992) 221.
[3] A. Atkinson, J.A. Hearne, C.F. Knights, Aqueous Chemistry and Thermodynamic Modelling of CaO–SiO_2–H_2O Gels, AERE R 12548, UKAEA, 1987.
[4] S. Börjesson, A. Emrén, C. Ekberg, Cem. Concr. Res. 27 (1997) 1649.
[5] M.M. Rahman, S. Nagasaki, S. Tanaka, Mater. Res. Soc. Symp. Proc. 556 (1999) 1237.
[6] M.M. Rahman, S. Nagasaki, S. Tanaka, Cem. Concr. Res. 29 (1999) 1091.
[7] D.A. Kulik, M. Kersten, J. Am. Ceram. Soc. 84 (2001) 3017.
[8] S.A. Greenberg, T.N. Chang, J. Phys. Chem. 69 (1965) 182.
[9] K. Fujii, W. Kondo, J. Am. Ceram. Soc. 66 (1983) C-220.
[10] K. Fujii, W. Kondo, J. Chem. Soc. Dalton. Trans. 2 (1981) 645.
[11] G.L. Kalousek, Proc 3rd Int Symp on Chem of Cements, London, 1954, p. 296.
[12] TRU Coordination Office (Japan Nuclear Cycle Development Institute and The Federation of Electric Power Companies), Progress Report on Disposal Concept for TRU Waste in Japan, JNC TY1400 2000-002, TRU TR-2000-02, 2000 (March).
[13] A. Atkinson, The time dependence of pH within a repository for radioactive waste disposal, AERE R 11777, UKAEA, 1985.
[14] H.F.W. Taylor, Cement Chemistry, 2nd ed., Thomas Telford Services Ltd, London, 1997.
[15] P.D. Glynn, Comput. Geosci. 17 (1991) 907.
[16] W. Stumm, J.J. Morgan, Aquatic Chemistry, 3rd ed., John Wiley & Sons, Inc., New York, 1996.

[17] A. Haworth, T.G. Heath, C.J. Tweed, HARPHRQ: a Computer Program for Geochemical Modelling, Nirex Report NSS/R380, 1995.
[18] K.A. Bond, T.G. Heath, C.J. Tweed, HATCHES: a Referenced Thermodynamic Database for Chemical Equilibrium Studies, Nirex Report NSS/R379, 1997.
[19] P. Faucon, J.M. Delaye, J. Virlet, J.F. Jacquinot, F. Adenot, Cem. Concr. Res. 27 (1997) 1581.
[20] D.E. Macphee, K. Luke, F.P. Glasser, E.E. Lachowski, J. Am. Ceram. Soc. 72 (1989) 646.
[21] F.P. Glasser, D.E. Macphee, E.E. Lachowski, Mater. Res. Soc. Symp. Proc. 112 (1988) 3.
[22] M.M. Rahman, T. Iwaida, S. Nagasaki, S. Tanaka, K. Haga, J. Nucl. Sci. Technol. 37 (2000) 793.